Talanta 85 (2011) 476–481

Contents lists available at ScienceDirect

Talanta

journal homepage: www.elsevier.com/locate/talanta

Gold nanorod-catalyzed luminol chemiluminescence and its selective determination of glutathione in the cell extracts of *Saccharomyces cerevisiae*

Chao Lu[a,*], Qianqian Li[a], Shuang Chen[a], Lixia Zhao[b], Zhixia Zheng[c]

[a] State Key Laboratory of Chemical Resource Engineering, Beijing University of Chemical Technology, Beijing 100029, China
[b] State Key Laboratory of Environmental Chemistry and Ecotoxicology, Research Center for Eco-Environmental Sciences, Chinese Academy of Sciences, Beijing 100085, China
[c] Provincial Key Laboratory of Research on Wastewater Treatment Technology, Anhui Academy of Environmental Science Research, Hefei 230022, China

ARTICLE INFO

Article history:
Received 3 February 2011
Received in revised form 30 March 2011
Accepted 5 April 2011
Available online 12 April 2011

Keywords:
Gold nanorods
Chemiluminescence
Glutathione
Saccharomyces cerevisiae

ABSTRACT

In this study, gold nanorods were firstly found to exhibit a tremendously higher catalytic activity towards luminol chemiluminescence (CL) than spherical gold nanoparticles. More importantly, ultra-trace aminothiols can cause a great CL decrease in the gold nanorod-catalyzed luminol system by the formation of Au–S covalent bonds on the ends of gold nanorods. Aminothiols can occupy the active sites of gold nanorods, and further interrupt the generation of the active oxygen intermediates. Other biomolecules including 19 standard amino acids, alcohols, organic acids and saccharides have no effect on gold nanorod-catalyzed luminol CL signals. Moreover, in order to evaluate the applicability and reliability of the proposed method, it was applied to the determination of glutathione in the cell extracts of *Saccharomyces cerevisiae*. Good agreements were obtained for the determination of glutathione in the cell extracts of *S. cerevisiae* between the present approach and a standard Alloxan method. The recoveries of glutathione were found to fall in the range between 96 and 105%. The calibration curve for glutathione was found to be linear from 0.05 to 100 nM, and the detection limit (S/N = 3) was 0.01 nM. The relative standard deviation (RSD) for five repeated measurements of 5.0 nM glutathione was 2.1%.

1. Introduction

Reduced glutathione is a major non-protein thiol compound, which seems to be involved in the response of different nutritional and oxidative stresses [1]. The intracellular glutathione content ranges from 1 to 15 mM [2]. Glutathione deficiency can cause aging and pathogenesis, and thus it is often used as a medicine for liver disease and a scavenger of the toxic compounds [1–4]. Glutathione preparation by *Saccharomyces cerevisiae* extract is an efficient approach as a supplement in food industry [5]. Therefore, a better understanding of glutathione content in yeast appears to be a basic need for microbial technology.

For the rapid determination of glutathione in the cell extracts of *S. cerevisiae*, the Alloxan method [6] is commonly used in food industry. But this method is elaborate, time-consuming, and the dynamic range is quite narrow (about one order of magnitude) with a high detection limit in the micromolar concentration order. Numerous other methods, such as fluorometric [7,8] and spectrophotometric [9] assays are available to quantify glutathione. Glutathione is absent of chromophores, and thus the chemical derivatization was required prior to analysis [10]. However, the usual derivatization is time-consuming and difficult to avoid the partial oxidation of glutathione.

Gold nanorods have received much attention due to their transverse (perpendicular) and longitudinal (parallel) surface plasmon resonance (SPR) absorption modes [11]. The transverse SPR band is located at about 520 nm, while the longitudinal SPR band is red-shifted to near-infrared regions (~900 nm). The changes of dielectric properties or refractive indices in surrounding medium can result in the different longitudinal SPR, which allows them to be extensively applied in chemical/biological sensing, imaging, drug delivery, and catalytic reactions [12,13].

The gold nanocrystal seed-mediated approach using cetyltrimethylammonium bromide (CTAB) as a stabilizing surfactant is commonly used to prepare large quantities of monodispersed gold nanorods, where CTAB surfactants take effect not only as rod-shape inducing agents, but also as capping agents. Therefore, the properties of gold nanorods strongly depend on the CTAB molecules on the surface of gold nanorods [14]. This makes gold nanorods more attractive in simple, rapid, ultrasensitive and selective sensing in a variety of biological species. However, the CTAB bilayer on the surface of gold nanorods cannot be easily displaced by biomolecules, and thus the applications of

* Corresponding author at: State Key Laboratory of Chemical Resource Engineering, Beijing University of Chemical Technology, Box 79, 15 Beisanhuan East Road, Beijing 100029, China. Tel.: +86 10 64411832; fax: +86 10 64411832.
E-mail addresses: luchao@mail.buct.edu.cn, luchao20022002@yahoo.com.cn (C. Lu).

0039-9140/$ – see front matter © 2011 Elsevier B.V. All rights reserved.
doi:10.1016/j.talanta.2011.04.013

CTAB-stabilized gold nanorods in biological sensing have not been widely pursued [15]. In recent years, there has been a great interest in the colorimetric detection of aminothiols using the aggregation of CTAB-stabilized gold nanorods [16–18]. For example, Sudeep and his co-workers [17] demonstrated the selective detection of micromolar concentrations of cysteine and glutathione from a pool of amino acids through a two-point electrostatic interaction between aminothiols in gold nanorods. More recently, Huang et al. [18] developed a sensitive and selective assay for cysteine by means of gold nanorods assemblies under acidic aqueous medium. However, the dynamic process of nanoparticle assemblies is strongly dependent on the surface charge, size and gold-based nanosensors, which results in a narrow linear range; moreover, the surrounding solvent environment and temperature have a great effect on nanoparticles assemblies, which should be carefully controlled in order to obtain reproducible assemblies. Therefore, it would be necessary to explore alternative methods to improve the advantages of gold nanorod-based sensor for the determination of aminothiols.

Chemiluminescence (CL) analysis has become increasingly important in various analytical fields for its high sensitivity, simple instrumentation, wide dynamic range and good reproducibility [19,20]. In recent years, CL has been extended to nanoparticle field from traditional molecular systems [21]. A variety of nanoparticles, such as gold, platinum, silver, bimetallic, semiconductor and magnetic nanoparticles, have been extensively utilized to enhance the different CL systems, however, almost all of nanoparticles involving in CL were spherical [22]. To the best of our knowledge, gold nanorod-catalyzed CL has been not reported.

In this study, it was found that gold nanorods can significantly catalyze the luminol CL, compared with spherical gold nanoparticles. Furthermore, it was found that aminothiols can greatly inhibit the gold nanorod-catalyzed luminol–H_2O_2 CL signals. Other amino acids and small biomolecules without thiol groups have no effect on the CL intensity of this proposed system. Based on this novel phenomenon, we investigated the inhibition effect of glutathione on the gold nanorod-catalyzed luminol–H_2O_2 CL signals, and the results showed that the inhibition CL intensity was proportional to the concentration of glutathione in the range from 0.05 to 100 nM. Therefore, a sensitive, accurate and rapid detection method for glutathione in the cell extracts of *S. cerevisiae* was established with satisfactory results.

2. Experimental

2.1. Reagents

Silver nitrate ($AgNO_3$), ascorbic acid, cetyltrimethylammonium bromide ($CH_3(CH_2)_{15}N(Br)(CH_3)_3$, CTAB) were purchased from Beijing Chemical Reagent Company (Beijing, China) without further purification. 20 standard amino acids, homocysteine and glutathione were obtained from Sigma–Aldrich (St. Louis, USA). Hydrogen tetrachloroaurate(III) trihydrate ($HAuCl_4{\cdot}3H_2O$), trisodium citrate dihydrate ($C_6H_5Na_3O_7{\cdot}2H_2O$) and sodium borohydride ($NaBH_4$) were purchased from Acros (Geel, Belgium). A 0.01 M stock solution of luminol (3-aminophthalhydrazide) was prepared by dissolving appropriate amounts of luminol (Acros, Geel, Belgium) in 0.1 M NaOH solution without purification. The storage of luminol leads to a stabilization of the luminol reactivity, and thus it was used after several weeks. Working solutions of luminol were prepared by diluting the stock solution with ultrapure water (Milli Q, Millipore, Barnstead, CA, USA). Working solutions of H_2O_2 were prepared daily from 30% (v/v) H_2O_2 (Beijing Chemical Reagent Company, Beijing, China). A 0.01 M stock solution of glutathione was prepared by dissolving appropriate amounts of glutathione in ultrapure water, and the working solution of glutathione was prepared by dilution of the stock solution. A glutathione-accumulated yeast strain *S. cerevisiae* Y-G-1 (Beijing, China) was used in this study. *Saccharomyces* culture medium and shake-flask culture conditions were prepared following the literature procedure [6]. All the reagents were of analytical grade, and all solutions were prepared with ultrapure water.

2.2. Apparatus

UV–vis spectra of gold nanorods were measured on a USB 4000 miniature fiber optic spectrometer in absorbance mode with a DH-2000 deuterium and tungsten halogen light source (Ocean Optics, Dunedin, FL). The centrifugation of gold nanorods was operated on a TGL-16B centrifugal machine (Shanghai Anting Scientific Instrument Factory, Shanghai, China). The sizes, shape and distribution of gold nanorods were confirmed through transmission electron microscopy (TEM) measurements using a Hitachi-800 TEM from Hitachi (Tokyo, Japan). The CL detection was conducted on a BPCL luminescence analyzer (Institute of Biophysics, Chinese Academy of Science, Beijing, China).

2.3. Synthesis of gold nanorods

Gold nanorods were prepared by a Ag(I)-assisted seed-mediated method using CTAB as template according to a previously reported method [23] with slight modifications as detailed. All glassware used for preparation of gold nanorods was thoroughly washed with freshly prepared aqua regia (HNO_3:HCl = 1:3), rinsed extensively with ultrapure water, and then dried in an oven at 100 °C for 2–3 h. An aqueous gold seed particle solution was prepared by adding 125 μL of 0.01 M $HAuCl_4$ to 4.875 mL of 0.1 M CTAB solution with gentle mixing. Next, 300 μL of freshly prepared, ice-cold 0.01 M $NaBH_4$ was added into this gold seed solution with stirring for 2 min. To avoid seed aging effects, the pale brown seed solutions were prepared not more than 4 h before use. Gold nanorods growth solution was prepared by adding the following reagents in order and then gently mixing at 25 °C: 95 mL of 0.1 M CTAB, 500 μL of 0.01 M $AgNO_3$, 5 mL of 0.01 M $HAuCl_4$, and 550 μL of 0.1 M ascorbic acid. The color of the solution was changed from colorless to brown-yellow and then to colorless. To initiate nanorod growth, 120 μL of the gold seed solution was added into the growth solution, and then capped the reaction vessel and slowly inverted it two times. After seed addition, the growth solution was maintained at 27 °C without stirring overnight. The spherical gold nanoparticles with average diameters of 38 nm were prepared following the literature procedure [24].

2.4. Spectral and TEM characterization of gold nanorods

UV–vis spectra of the synthesized gold nanorods were obtained by direct determination of the growth solution. Prior to the TEM preparation, excess CTAB was removed from the suspension by dilution with ultrapure water followed by 10 min centrifugation at 13,000 × g (repeated 3 times). The TEM specimens were prepared by depositing an appropriate amount of the concentrated gold nanorods onto the carbon-coated copper grids, and excess solution was wicked away by a filter paper. The grid was subsequently dried in air before measure. As shown in Fig. 1, the average length and width of the gold nanorods were ~55.0 nm and ~18.4 nm, respectively, and a longitudinal plasmon resonance at 708 nm was obtained by the above procedure. Assuming nanoparticle density equivalent to that of bulk gold (19.30 g/cm^3), the concentration of the as-prepared gold nanorods and 38 nm spherical gold nanoparticles was calculated to be ~0.58 nM and ~0.15 nM, respectively.

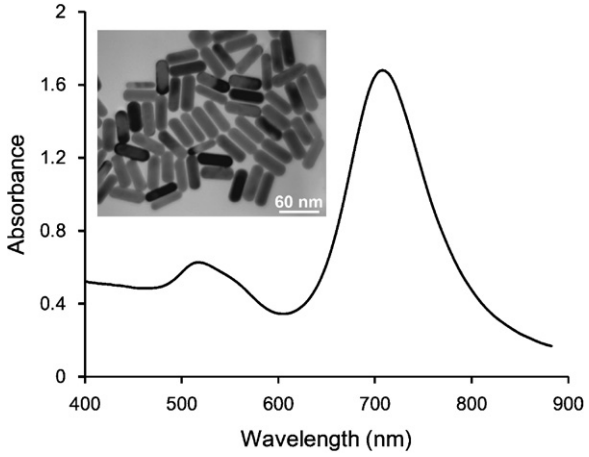

Fig. 1. UV–vis absorption spectra of gold nanorods; inset, TEM of gold nanorods.

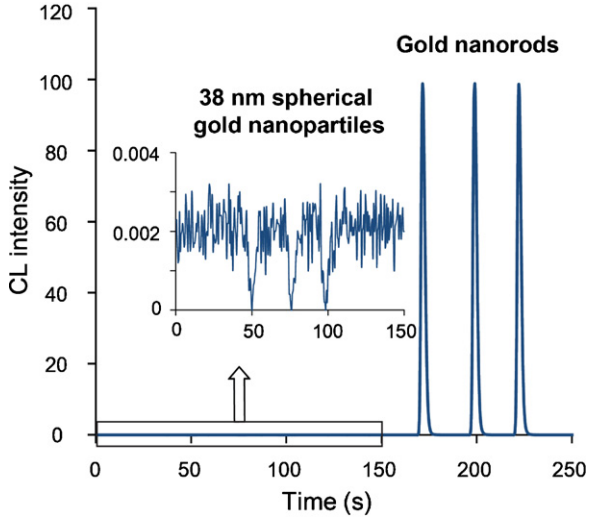

Fig. 3. CL intensity of luminol–H_2O_2 in the presence of 38 nm spherical gold nanoparticles or gold nanorods at the same concentration (0.15 nM).

2.5. Procedures for CL detection

For the signal comparability, we used the flow injection analysis (Fig. 2). When the catalytic activity of gold nanorods on the luminol–H_2O_2 CL system was investigated, the gold nanorods solution was injected into the carrier stream (ultrapure water) through a 100 μL loop-valve injector, mixed with solution A (ultrapure water), 1.0 μM luminol in 1.0 mM NaOH, and 2.0 mM H_2O_2 through three-way pieces. Then, the mixed solution flowed via a spiral-shaped flow cell positioned in front of a photomultiplier tube (PMT) operating at −950 V, and the PMT signals were imported to the computer for data acquisition. When the inhibition effects of aminothiols on the CL system were investigated, solution A was changed to aminothiol solutions and mixed with gold nanorods before reacting with luminol and H_2O_2. The variation in CL intensity of gold nanorod-catalyzed luminol resulting from aminothiols can be described as $\Delta I = I_0 - I$, where I_0 is the CL signal in the absence of aminothiols and I is the CL signal in the presence of aminothiols.

3. Results and discussion

3.1. Enhancement of gold nanorods on luminol CL

In this work, at the same concentration (0.15 nM), the catalytic effect of gold nanorods on the luminol–H_2O_2 CL was compared with that of 38 nm spherical gold nanoparticles by a flow injection system. The results shown in Fig. 3 indicated the CL signal of the luminol–H_2O_2 system was significantly enhanced by gold nanorods; while 38 nm spherical gold nanoparticles have no effect on luminol–H_2O_2 CL intensity. Interestingly, it was reported that the most intensive CL signals were obtained with 38 nm spherical gold nanoparticles-catalyzed luminol–H_2O_2 CL intensity [25]. This disagreement was due to that the optimum concentrations of luminol and H_2O_2 in our study were 1.0 μM and 2.0 mM, respectively; while 200 μM luminol and 10 mM H_2O_2 were chosen in reference 25. Therefore, the consumption of the reagents was much lower in our study.

In order to confirm the main contribution to the enhancement of luminol CL, the coexisting substances in preparation of gold nanorods, including $AgNO_3$, CTAB, $HAuCl_4$, $NaBH_4$ and ascorbic acid were investigated, and the results were shown in Table 1. Note that the as-prepared gold nanorods were purified by 3 centrifugation washes before they were injected into the flow injection system, and thus the concentrations of these coexisting substances in preparation of gold nanorods were so low (see Table 1) that their influence on the CL intensity was negligible. It was concluded that the main source in the enhancement of the luminol CL was gold nanorods instead of spherical gold nanoparticles and coexisting substances. It is well-known that the catalytic activity of metal nanoparticles depends on their shape, and gold nanorods possess higher surface-to-volume ratio, higher electron density and lower activation energy than spherical nanoparticles [26–28]. Therefore, gold nanorods have a higher catalytic activity than spherical gold nanoparticles, resulting in a significant enhancement on the luminol CL intensity as depicted in Fig. 4a. The similar finding was reported by Li and his co-workers, where they demonstrated the catalytic efficiency of the irregular gold nanoparticles on luminol

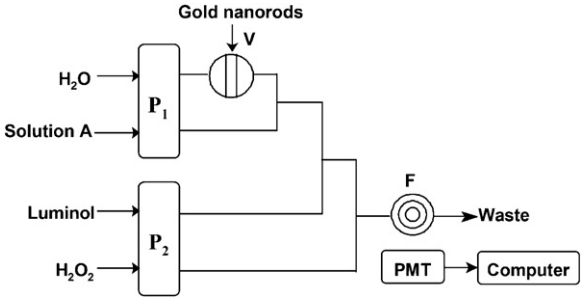

Fig. 2. Schematic diagram of CL detection by flow injection system. P_1 and P_2, peristaltic pumps; V, a six-channel injection valve (100 μL); F, flow cell (1.0 mm i.d. × 50.0 cm length); PMT, photomutiplier tube. Experimental conditions: the flow rates of P_1 and P_2 were 3.0 mL/min and 1.0 mL/min, respectively; the concentrations of gold nanorods, luminol, NaOH and H_2O_2 were 0.5 nM, 1.0 μM, 1.0 mM and 2.0 mM, respectively.

Table 1
The tolerable concentration of some coexisting substances in preparation of gold nanorods solution to the luminol–H_2O_2 system.

Substances	Tolerance (M)	Original concentration (M)[a]	Working concentration (M)[b]
$AgNO_3$	5×10^{-6}	5×10^{-5}	5×10^{-9}
CTAB	10^{-3}	10^{-1}	10^{-5}
$HAuCl_4$	10^{-6}	5×10^{-4}	5×10^{-8}
$NaBH_4$	10^{-4}	7.2×10^{-7}	7.2×10^{-11}
Ascorbic acid	10^{-7}	5.5×10^{-4}	5.5×10^{-8}

[a] The original concentration of the substances in preparation of gold nanorods.
[b] The working concentration of the substances in the gold nanorods solution after the as-prepared gold nanorods were purified by 3 centrifugation washes.

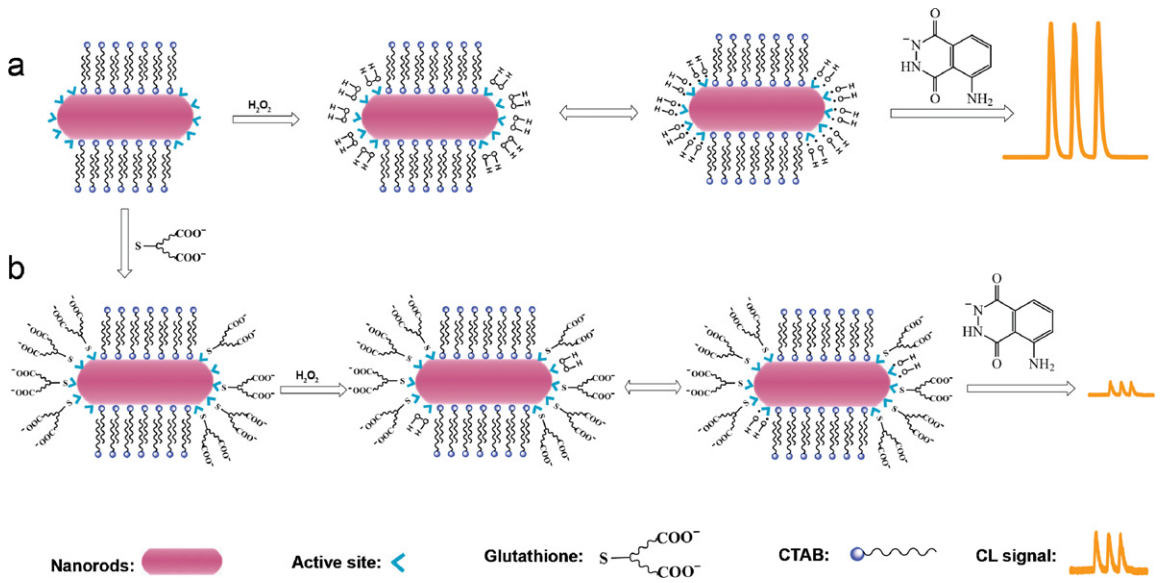

Fig. 4. Schematic illustration of (a) catalytic activity of gold nanorods on luminol CL; (b) the inhibition of glutathione on luminol–H_2O_2–gold nanorods CL.

CL was 100-fold greater than that of spherical gold nanoparticles [29].

3.2. Inhibition effect of aminothiols on gold nanorod-catalyzed luminol CL

We investigated the CL changes of the as-prepared gold nanorod-catalyzed luminol reaction upon the addition of a variety of biomolecules including three aminothiols (*i.e.*, cysteine, homocysteine and glutathione), 19 standard amino acids, alcohols, organic acids and saccharides. As shown in Fig. 5, the results indicated that the CL intensity significantly decreased upon the addition of 10 nM cysteine, homocysteine or glutathione; however, no CL change occurred in the presence of the mixed amino acids, alcohols, organic acids and saccharides (each 1.0 μM). It was reported that the CTAB-stabilized gold nanorods were single-crystalline with their side faces enclosed by the {1 0 0} and {1 1 0} facets, and {1 1 1} crystalline end faces. The CTAB bilayer on gold nanorods made macromolecular compounds inaccessible to the {1 0 0} and {1 1 0} side faces of gold nanorods [30–33]. However, thiols compounds can strongly interact with the {1 1 1} end faces of gold nanorods by the formation of Au–S covalent bonds, taking up the active sites of the gold nanorods [16,34,35]. Therefore, only aminothiols (*e.g.*, glutathione as depicted in Fig. 4b) can cause a great decrease in the CL intensity of the gold nanorod-catalyzed luminol–H_2O_2 system.

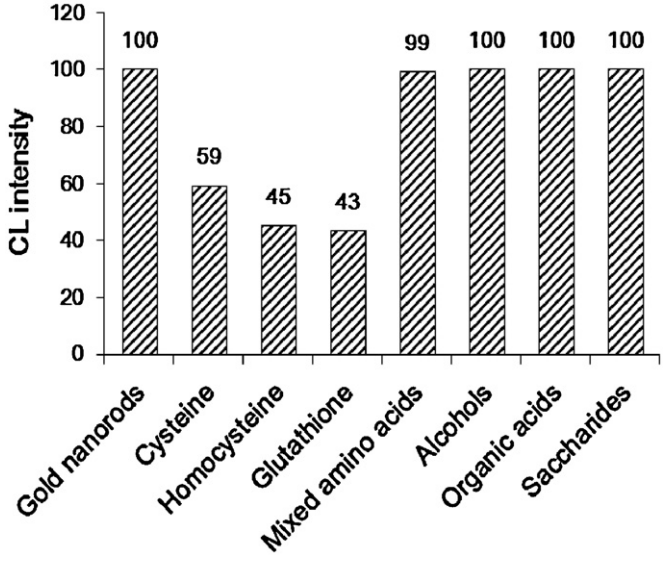

Fig. 5. The CL inhibition of the luminol–H_2O_2–gold nanorods system by adding different compounds: 10 nM cysteine, homocysteine, glutathione; mixed amino acids containing alanine, cystine, valine, histidine, asparagines, serine, aspartic acid, tryptophan, isoleucine, lysine, proline, methionine, tyrosine, arginine, threonine, leucine, phenylalanine, glutamic acid and glycine; alcohols containing 1,2-propanediol, glycerol, 1,2,3-butanetriol, 3-deoxy-D-mannitol and glucitol; organic acids containing lactic acid, succinic acid, fumaric acid, pentanedioic acid, oxalacetic acid and pyruvic acid; saccharides containing sucrose, maltose and glucose (1.0 μM each).

3.3. Optimization conditions for the CL detection of glutathione

To demonstrate the practicability of the as-prepared gold nanorod-catalyzed luminol CL reaction in bioassays, the effects of various experimental conditions on the relative CL intensity were investigated using glutathione as a model thiol compound.

3.3.1. Concentration of gold nanorods

In this study, gold nanorods acted as an efficient catalyst of the luminol CL. Therefore, the concentration of gold nanorods played a key role on the luminol CL. As shown in Fig. 6a, the effect of the concentration of gold nanorods in the range of 0.2–0.8 nM on the luminol CL was investigated. The CL intensity (I_0 and I) increased steadily with increasing the concentration of gold nanorods in the presence or absence of glutathione. Considering the relative CL intensity and the consumption of the reagents, 0.5 nM was selected as the optimal concentration of gold nanorods.

3.3.2. Selection of flow rate

In the absence of glutathione, the CL intensity (I_0) linearly increased along with the increased flow rate of pump 1 (P_1, for carrier water and sample solution) in the range 1.0–3.0 mL/min; while the CL intensity (I) was almost constant in the presence of glutathione (Fig. 6b). Therefore, the optimized flow rate of P_1 was 3.0 mL/min in term of the relative CL intensity and the consumption of the reagents. Similarly, we investigated the effects of the flow rate of pump 2 (P_2, for luminol and H_2O_2 solutions) on the relative

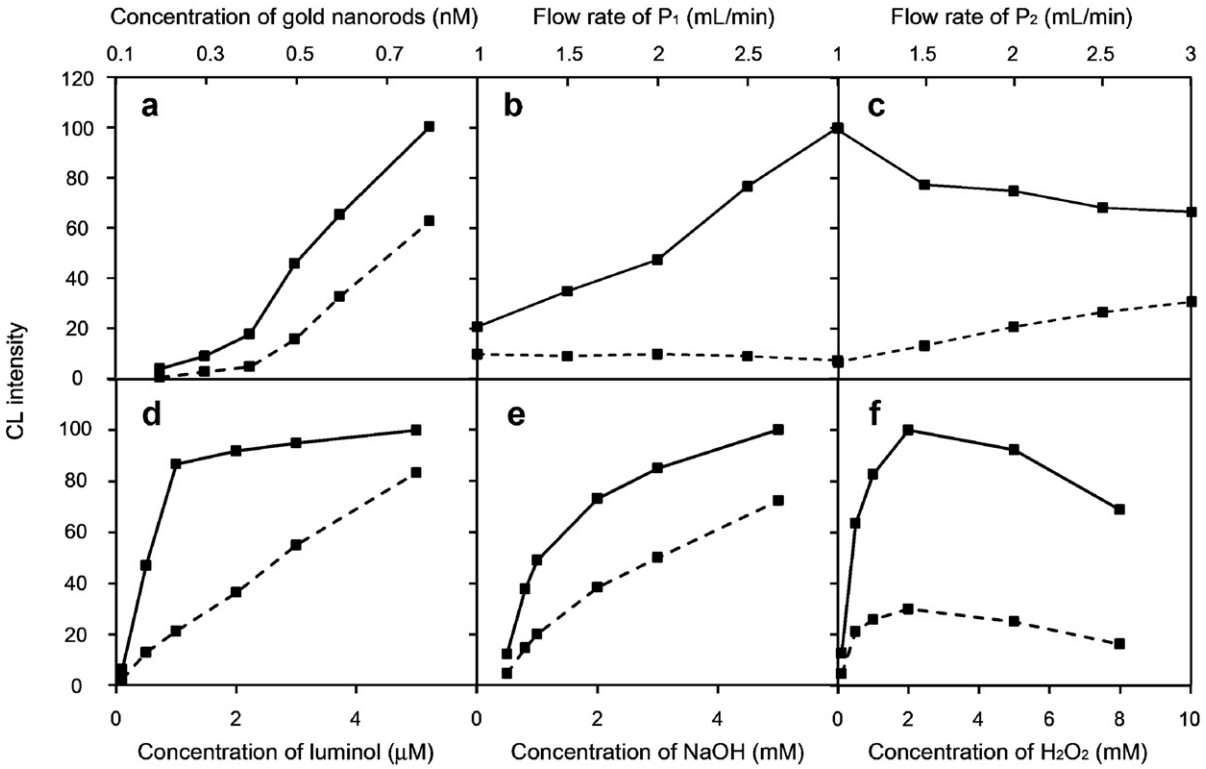

Fig. 6. Effects of the reaction conditions on the gold nanorod-catalyzed luminol CL in the absence (solid line) and the presence (dashed line) of 0.1 μM glutathione: (a) concentration of gold nanorods: the flow rates of P_1 and P_2 were 3.0 mL/min and 1.0 mL/min, respectively; the concentrations of luminol, NaOH and H_2O_2 were 1.0 μM, 1.0 mM and 2.0 mM, respectively; (b) flow rate of P_1: the flow rate of P_2 was 1.0 mL/min; the concentrations of gold nanorods, luminol, NaOH and H_2O_2 were 0.5 nM, 1.0 μM, 1.0 mM and 2.0 mM, respectively; (c) flow rate of P_2: the flow rate of P_1 was 3.0 mL/min; the concentrations of gold nanorods, luminol, NaOH and H_2O_2 were 0.5 nM, 1.0 μM, 1.0 mM and 2.0 mM, respectively; (d) concentration of luminol: the flow rates of P_1 and P_2 were 3.0 mL/min and 1.0 mL/min, respectively; the concentrations of gold nanorods, NaOH and H_2O_2 were 0.5 nM, 1.0 mM and 2.0 mM, respectively; (e) concentration of NaOH: the flow rates of P_1 and P_2 were 3.0 mL/min and 1.0 mL/min, respectively; the concentrations of gold nanorods, luminol and H_2O_2 were 0.5 nM, 1.0 μM and 2.0 mM, respectively; (f) concentration of H_2O_2: the flow rates of P_1 and P_2 were 3.0 mL/min and 1.0 mL/min, respectively; the concentrations of gold nanorods, luminol and NaOH were 0.5 nM, 1.0 μM and 1.0 mM, respectively.

CL intensity at 3.0 mL/min for P_1. As shown in Fig. 6c, 1.0 mL/min was selected as the optimal flow rate of P_2 in this study.

3.3.3. Concentration of luminol

The concentration of luminol was a key parameter for the luminol CL. In this paper, the effect of the concentration of luminol on the relative CL intensity was investigated in the range of 0.1–5.0 μM (Fig. 6d). In the absence of glutathione, the most suitable CL intensity was observed at 1.0 μM luminol; however, the CL intensity increased steadily with increasing concentration of luminol in the presence of glutathione. The CL intensity difference was maximal when the concentration of luminol was 1.0 μM, which was chosen in further experiments.

3.3.4. Concentration of sodium hydroxide

It is well known that the luminol CL reaction occurs in alkaline mediums, and aqueous NaOH solution is often used for dissolving luminol and adjusting the pH of luminol solutions [20]. In this study, we investigated the concentration of NaOH in the range of 0.5–5.0 mM. As shown in Fig. 6e, the CL intensity increased with increasing concentrations of NaOH in the presence or absence of glutathione. 1.0 mM NaOH was used as the optimum concentration due to the achievement of high detection sensitivity and low background signals. Note that the pH of the working solution of 1.0 μM luminol in 1.0 mM NaOH solution was 10.9.

3.3.5. Concentration of hydrogen peroxide

Concentration of H_2O_2 on the relative CL intensity was examined in the range of 0.5–8.0 mM. Without H_2O_2 in the reaction, there was no CL emission observed. As shown in Fig. 6f, the relative CL intensity was the strongest when the concentration of H_2O_2 was 2.0 mM. The concentrations of H_2O_2 higher or lower than 2.0 mM caused a decrease in the relative CL intensity. Therefore, this system was operated at 2.0 mM H_2O_2 throughout this study.

3.4. Standard curve and detection limit

Under the optimum experimental conditions employed in the present study, the calibration curve was found to be linear from 0.05 to 100 nM for glutathione (Fig. 7). The regression equation was $\log \Delta I = 0.2652 \log C + 3.8603$ ($R^2 = 0.9969$), where ΔI is the relative CL intensity and C is the concentration of glutathione. The limit of detection (LOD) for glutathione (S/N = 3) was 0.01 nM. The relative standard deviation for five repeated measurements of 5.0 nM glutathione was 2.1%. The time of analysis for each sample is about 20 s.

3.5. Real samples

In order to evaluate the applicability of the gold nanorod-catalyzed luminol CL reaction in the analysis of real samples, the system was applied to detect glutathione in the cell extracts of *S. cerevisiae*. Note that there is very low cysteine or no homocysteine content in the cell extracts of *S. cerevisiae* [5,6,10]. The analytical merits of the present method were evaluated by comparing with the standard Alloxan method [6]. The calibration curve was obtained by standard addition method, which was used for the determination of glutathione in the cell extracts of *S. cerevisiae*

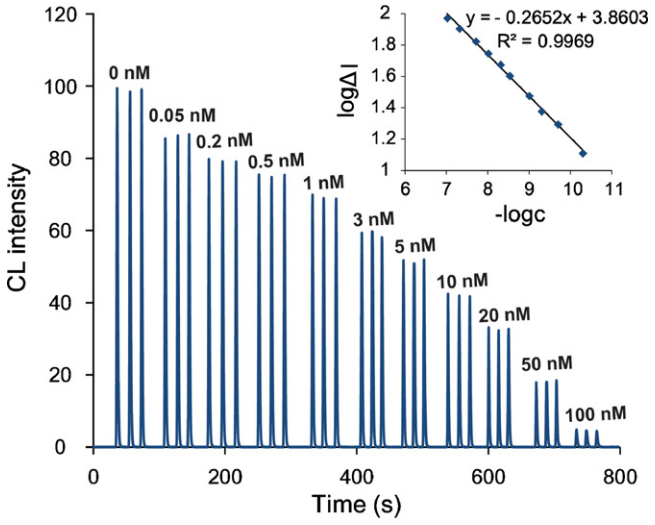

Fig. 7. The CL inhibition of the gold nanorod-catalyzed luminol CL by adding different concentrations of glutathione; inset, calibration curve for standard glutathione, $\Delta I = I_0 - I$, showed the effect of glutathione on the CL intensity of the system, where I_0 stands for the signal in the absence of glutathione and I stands for the signal in the presence of glutathione.

Table 2
Determination of glutathione in the cell extracts of *Saccharomyces cerevisiae*.

Sample	UV–vis method (μM)[a]	CL method (μM)[a]	Added (μM)	Found (μM)[a]	Recovery (%)
1	3.0 ± 0.02	2.8 ± 0.04	2.0	2.1 ± 0.05	105 ± 2.5
			5.0	4.9 ± 0.07	99 ± 1.4
2	6.5 ± 0.05	5.9 ± 0.07	5.0	5.2 ± 0.06	104 ± 1.2
			10.0	9.8 ± 0.09	98 ± 0.9
3	16.5 ± 0.09	17.8 ± 0.11	10.0	9.6 ± 0.07	96 ± 0.7
			15.0	15.3 ± 0.09	102 ± 0.6

[a] Mean ± SD of three measurements.

(Table 2). The results of the present CL method were in good agreement with that obtained by the standard Alloxan method. Note that the differences between the standard Alloxan method and the proposed CL method were higher than 5% for glutathione content in the cell extracts of *S. cerevisiae*. This may be attributed to the longer analysis time of the standard Alloxan method (about 20 min).

4. Conclusions

In this study, based on glutathione-inhibited gold nanorod-catalyzed luminol CL, a novel assay method for glutathione in the cell extracts of *S. cerevisiae* was successfully developed. To the best of our knowledge, this is the first work to use gold nanorod-based CL sensors for determination for analytes. Moreover, the gold nanorod-catalyzed luminol CL system exhibited its potential in analytical applications for aminothiols sensing in a variety of samples, which will be our next experimental scheme.

Acknowledgements

This work was financially supported by the National Natural Science Foundation of China (Nos. 21077008, 20975010 and 20907060) and International Science and Technology Cooperation Project (Nos. 2008DFA91310 and 2009DFA93030) from Ministry of Science and Technology of China.

References

[1] M. Penninckx, Enzyme Microb. Technol. 26 (2000) 737–742.
[2] Y.C. Hou, Z.M. Guo, J. Li, P.G. Wang, Biochem. Biophys. Res. Commun. 228 (1996) 88–93.
[3] A. Pastore, G. Federici, E. Bertini, F. Piemonte, Clin. Chim. Acta 333 (2003) 19–39.
[4] J.F. Wu, J.P. Ferrance, J.P. Landers, S.G. Weber, Anal. Chem. 82 (2010) 7267–7273.
[5] Z. Wang, L.Y. Zhang, T.W. Tan, Process Biochem. 45 (2010) 1168–1171.
[6] S.H. Wen, T. Zhang, T.W. Tan, Process Biochem. 40 (2005) 3474–3479.
[7] B.C. Zhu, X.L. Zhang, H.Y. Jia, Y.M. Li, S.T. Chen, S.C. Zhang, Dyes Pigments 86 (2010) 87–92.
[8] E. Causse, C. Issac, P. Malatray, C. Bayle, P. Valdiguie, R. Salvayre, F. Couderc, J. Chromatogr. A 895 (2000) 173–178.
[9] A.R.T.S. Araujo, M.L.M.F.S. Saraiva, J.L.F.C. Lima, Talanta 74 (2008) 1511–1519.
[10] P. Monostori, G. Wittmann, E. Karg, S. Túri, J. Chromotogr. B 877 (2009) 3331–3346.
[11] V. Sharma, K. Park, M. Srinivasarao, Mater. Sci. Eng. R 65 (2009) 1–38.
[12] R. Becker, B. Liedberg, P.-O. Käll, J. Colloid Interface Sci. 343 (2010) 25–30.
[13] R.X. Zou, Q. Zhang, Q. Zhao, F. Peng, H.J. Wang, H. Yu, J. Yang, Colloids Surf. A: Physicochem. Eng. Aspects 372 (2010) 177–181.
[14] J. Perez-Juste, I. Pastoriza-Santos, L.M. Liz-Marzan, P. Mulvaney, Coord. Chem. Rev. 249 (2005) 1870–1901.
[15] H.W. Huang, X.Y. Liu, Y.L. Zeng, X.Y. Yu, B. Liao, P.G. Yi, P.K. Chu, Biomaterials 30 (2009) 5622–5630.
[16] C. Li, C.L. Wu, J.S. Zheng, J.P. Lai, C.L. Zhang, Y.B. Zhao, Langmuir 26 (2010) 9130–9135.
[17] P.K. Sudeep, S.T.S. Joseph, K.G. Thomas, J. Am. Chem. Soc. 127 (2005) 6516–6517.
[18] H.W. Huang, X.Y. Liu, T. Hu, P.K. Chu, Biosens. Bioelectron. 25 (2010) 2078–2083.
[19] C. Lu, J.G. Li, Y. Yang, J.-M. Lin, Talanta 82 (2010) 1576–1580.
[20] C. Lu, G.Q. Song, J.-M. Lin, Trends Anal. Chem. 25 (2006) 985–995.
[21] D.L. Giokas, A.G. Vlessidis, G.Z. Tsogas, N.P. Evmiridis, Trends Anal. Chem. 29 (2010) 1113–1126.
[22] Q.Q. Li, L.J. Zhang, J.G. Li, C. Lu, Trends Anal. Chem. 30 (2011) 402–413.
[23] L.F. Gou, C.J. Murphy, Chem. Mater. 17 (2005) 3668–3672.
[24] C. Lu, N. Zhang, J.G. Li, Q.Q. Li, Talanta 81 (2010) 698–702.
[25] Z.-F. Zhang, H. Cui, C.-Z. Lai, L.-J. Liu, Anal. Chem. 77 (2005) 3324–3329.
[26] R. Narayanan, M.A. El-Sayed, J. Phys. Chem. B 109 (2005) 12663–12676.
[27] R. Narayanan, M.A. El-Sayed, Nano Lett. 4 (2004) 1343–1348.
[28] X.C. Zhou, W.L. Xu, G.K. Liu, D. Panda, P. Chen, J. Am. Chem. Soc. 132 (2010) 138–146.
[29] Z.P. Wang, J.Q. Hu, Y. Jin, X. Yao, J.H. Li, Clin. Chem. 52 (2006) 1958–1961.
[30] H.W. Liao, J.H. Hafner, Chem. Mater. 17 (2005) 4636–4641.
[31] J.X. Gao, C.M. Bender, C.J. Murphy, Langmuir 19 (2003) 9065–9070.
[32] C.K. Tsung, X.S. Kou, Q.H. Shi, J.P. Zhang, M.H. Yeung, J.F. Wang, G.D. Stucky, J. Am. Chem. Soc. 128 (2006) 5352–5353.
[33] M.Z. Liu, P. Guyot-Sionnest, J. Phys. Chem. B 109 (2005) 22192–22200.
[34] P.R. Selvakannan, E. Dumas, F. Dumur, C. Péchoux, P. Beaunier, A. Etcheberry, F. Sécheresse, H. Remita, C.R. Mayer, J. Colloid Interface Sci. 349 (2010) 93–97.
[35] X.S. Kou, S.Z. Zhang, Z. Yang, C.K. Tsung, G.D. Stucky, L.D. Sun, J.F. Wang, C.H. Yan, J. Am. Chem. Soc. 129 (2007) 6402–6404.